

FOURTEENTH EUROPEAN ROTORCRAFT FORUM

Paper No. 57

**A MODEL FOR ACTIVE CONTROL
OF HELICOPTER AIR RESONANCE IN
HOVER AND FORWARD FLIGHT**

M.D. TAKAHASHI AND P.P. FRIEDMANN

**MECHANICAL, AEROSPACE AND NUCLEAR ENGINEERING DEPARTMENT,
UNIVERSITY OF CALIFORNIA, LOS ANGELES,
LOS ANGELES, CALIFORNIA 90024-1597 U.S.A.**

20-23 September, 1988

MILANO, ITALY

**ASSOCIAZIONE INDUSTRIE AEROSPAZIALI
ASSOCIAZIONE ITALIANA DI AERONAUTICA ED ASTRONAUTICA**

A MODEL FOR ACTIVE CONTROL OF HELICOPTER AIR RESONANCE IN HOVER AND FORWARD FLIGHT

M.D. Takahashi* and P.P. Friedmann**
Mechanical, Aerospace, and Nuclear Engineering Department
University of California
Los Angeles, California 90024

Abstract

A coupled rotor/fuselage helicopter analysis is presented. The accuracy of the model is verified by comparing it with the experimental data. The sensitivity of the open loop damping of the unstable air resonance mode to such modeling effects as blade torsional flexibility, unsteady aerodynamics, forward flight, periodic terms, and trim solution is illustrated by numerous examples. Subsequently, the model is used in conjunction with linear optimal control theory to stabilize the air resonance mode. The influence of the modeling effects mentioned before on active air resonance control is then investigated.

Nomenclature

Most of the variables in this paper are in *non-dimensional* form. Any dimensional variables are represented with an overbar. Unless otherwise stated, recovery of the dimensional values from the non-dimensional values is done by multiplying the variable by the correct dimensional combination of characteristic mass, length, and time are blade mass, rotor radius, and inverse of the rotor rotation rate.

a	Rotor blade lift curve slope
a_T	Horizontal tail lift curve slope
A, B, C	System, control, and output matrices
AR	Horizontal tail aspect ratio
b	Blade semi-chord
C_{d0}	Blade drag coefficient
C_{dOT}	Horizontal tail drag coefficient
C_{Mx}, C_{My}	Roll and Pitch Coefficient = $\frac{\text{Moment}}{\pi \bar{R}^2 \bar{\rho} \bar{R}^2 \bar{\Omega}^2}$

*Presently Research Scientist, U.S. Army Aeroflightdynamics Laboratory, Moffett Field, CA.

**Professor and Chairman

C_T	Thrust coefficient = $\frac{\text{Thrust}}{\pi \bar{R}^2 \bar{\rho}_A \bar{R}^2 \bar{\Omega}^2}$
C_W	Weight coefficient = $\frac{\text{Total Weight}}{\pi \bar{R}^2 \bar{\rho}_A \bar{R}^2 \bar{\Omega}^2}$
e	Hinge offset
f	Fuselage drag area = $\frac{\bar{f}}{2\bar{b}\bar{r}}$
f_b, f_t	Column vectors of blade and fuselage equations for trim and equilibrium solution generation
f_{b0}, f_{bnc}, f_{bns} f_{t0}, f_{tnc}, f_{tns}	Column vectors of coefficients of the Fourier expansion of f_b and f_t
H, R	Weight matrices of regulator problem
I_b	Blade flap inertia about hinge offset
$I_{Cxx}, I_{Cyy}, I_{Czz}$	Fuselage mass moments of inertia about the fuselage center of mass
J_x	Blade pitch inertia
J_y, J_z	Integral of the blade flap and lead-lag bending inertias
K_c	Feedback gain matrix
K_x, K_y, K_z	Blade spring constants
l	Blade length
\bar{M}_B	Dimensional blade mass
M_F	Fuselage mass
$M_{\lambda\lambda}, L^{-1}$	Dynamic inflow matrices
N_b	Number of blades
N_{DOF}	Number of blade degrees of freedom
N_H	Number of harmonics
q	System Degrees of Freedom
q_b, q_t	Column vectors of blade equilibrium solution and trim variables
q_{b0}, q_{bnc}, q_{bns}	Column vectors of coefficients of the Fourier expansion of q_b
P_c	Positive semi-definite solution to the regulator of Riccati equation
r	Distance from rotor hub center
\bar{R}	Dimensional rotor radius
R_c	Elastic coupling coefficient
R_{Mx}, R_{My}, R_{Mz}	Translational degrees of freedom of point M on the helicopter
S_T	Horizontal tail area

x	State vector $[q^T \dot{q}^T]^T$
x_A	Blade aerodynamic center offset from the blade elastic axis
x_b, y_b, z_b	Position of blade center of mass from the hinge offset
$\hat{x}_1, \hat{y}_1, \hat{z}_1$	Body fixed triad
X_{MC}, Z_{MC}	X and Z position of the fuselage center of mass from point M on the helicopter
X_{MH}, Z_{MH}	X and Z position of the rotor hub center from point M on the helicopter
X_{MT}, Z_{MT}	X and Z position of the horizontal tail aerodynamic center from point M
u	Input vector $[\Delta\theta_0, \Delta\theta_{1s}, \Delta\theta_{1c}]^T$
V	Vehicle forward flight speed
α_R	Rotor plane trim pitch angle (positive nose down)
β_p	Blade precone angle
β_k, ζ_k, ϕ_k	The k^{th} blade rotating flap, lead-lag, and torsional degrees of freedom
$\beta_{1c}, \zeta_{1c}, \phi_{1c}$	Non-rotating cosine flap, lead-lag, and torsional degrees of freedom
$\beta_{1s}, \zeta_{1s}, \phi_{1s}$	Non-rotating sine flap, lead-lag, and torsional degrees of freedom
γ	Lock number
$\theta_0, \theta_{1s}, \theta_{1c}$	Collective, sine, and cosine inputs
$\theta_x, \theta_y, \theta_z$	Roll, pitch and yaw degrees of freedom
θ_{pk}	Pitch of k^{th} blade $\bar{V} \sin(\alpha_R)$
λ_{fs}	Free stream inflow = $\frac{\bar{V} \sin(\alpha_R)}{R\bar{\Omega}}$
λ_i	Induced flow
$\lambda_0, \lambda_c, \lambda_s$	Dynamic inflow perturbations
λ	Total constant inflow = $\lambda_{fs} + \lambda_i$
λ_k	Total inflow $\frac{\bar{V} \cos(\alpha_R)}{R\bar{\Omega}}$
μ	Advance ratio = $\frac{\bar{V} \cos(\alpha_R)}{R\bar{\Omega}}$
ρ_A	Air density $\frac{2N_b b}{\pi}$
σ	Solidity ratio = $\frac{2N_b b}{\pi}$
ψ_k	k^{th} blade angle = $\frac{2\pi}{N_b}(k-1)$
ψ	Azimuth angle of blade measured from straight aft position
$\omega_{F1}, \omega_{L1}, \omega_{T1}$	Rotating first flap, lag, and torsional blade frequencies
Ω	Dimensional rotor rate

Introduction

The desire to reduce the mechanical complexity and weight of the rotor hub on helicopters has generated considerable interest in hingeless and bearingless rotors. Though these new rotor configurations are simple and lightweight they can introduce other undesirable dynamic problems. One potential instability, denoted "air resonance", is a condition where the blade lead-lag motions strongly interact with the fuselage pitch or roll motions in flight [1,2]. This aeromechanical phenomenon produces large fuselage oscillations and is clearly undesirable when unstable or weakly stable. One possible means of stabilizing or augmenting stability of air resonance is through an active controller. Research in this area has been limited to a few references [3,4,5], where various theoretical active control studies are presented. The helicopter models used in these studies had considerable limitations. Important effects such as torsional flexibility in the rotor blades, forward flight, and unsteady aerodynamic effects are all missing from these models. Clearly, any conclusions drawn from a control study are only as good as the model used to generate them. Thus, the *first objective* of this research is to accurately model the coupled rotor/fuselage air resonance problem in forward flight including the important effects of the rotor blade torsional flexibility and unsteady aerodynamics. Naturally, after doing this, one would like to demonstrate the feasibility of actively controlling air resonance throughout the wide range of operating conditions that a helicopter encounters. However, before this can be done a fundamental understanding of what constitutes a reasonable control design model and how the controller interacts with the system is necessary. This leads to the *second objective* of this paper, which is to evaluate the importance of various modeling effects in actively controlling air resonance.

Mathematical Model

Due to the complexity of the coupled rotor/fuselage problem, certain simplifications in the analysis are necessary for the problem to be tractable. The primary emphasis of this paper is on the basic problem of controlling air resonance in forward flight. Therefore, a simple offset hinged spring restrained blade model is used to represent a hingeless rotor blade (Figure 1). This assumption simplifies the equations of motion, while retaining the essential features of the air resonance problem [1]. In this model, the blade elasticity is concentrated at a single point called the hinge offset point, and torsional springs are used to represent this flexibility. By setting the flapping and lead-lag spring constants equal to zero, this model can also be used to represent articulated blades. The dynamic behavior of the rotor blade is represented by three degrees of freedom for each blade, which are flap, lag, and torsion motions. The fuselage is represented as a rigid body with five degrees of freedom, where three of these are linear translations and two are angular positions of pitch and roll (Figure 2). Yaw is ignored since its effect in the air resonance problem is known to be small. The formulation is such that the translational degrees of freedom of the fuselage can be chosen freely. Thus, the model can represent both a helicopter in flight as well as a mounted configuration such as in a wind tunnel test.

The active control of the system is implemented through a conventional swashplate, thus the pitch of the k^{th} rotor blade is given by the expression

$$\theta_{pk} = (\theta_0 + \Delta\theta_0) + (\theta_{1c} + \Delta\theta_{1c})\cos(\psi_k) + (\theta_{1s} + \Delta\theta_{1s})\sin(\psi_k) \quad (1)$$

The Δ terms are the small active control inputs and the terms without Δ are the rotor trim inputs necessary to satisfy the trim conditions of the helicopter, which for this paper, is restricted to the case of straight and level flight.

The aerodynamic loads of the rotor blades are based on Greenberg's theory, which is a two dimensional strip theory [6,7]. Compressibility and dynamic stall effects are neglected, though they could be important at high advance ratios. Greenberg's theory is an extension of Theodorsen theory, which accounts for a time-dependent lead-lag motion and constant collective pitch of the blade. A time domain extension of this theory, presented in Ref. 8, is capable of capturing unsteady aerodynamic effects, which are created by the time dependent wake shed by the airfoil as it undergoes arbitrary time dependent motion. However, since air resonance is a relatively low frequency instability, the use of a dynamic inflow model is deemed to be adequate for capturing unsteady aerodynamic effects. References 9 and 10 have shown that this model is suitable for representing the low frequency unsteady aerodynamic effects, in hover and forward flight, required for the analysis of coupled rotor/fuselage configurations, in air resonance.

Dynamic inflow is based on the assumption that the total inflow through the rotor plane is given by

$$\lambda_k = \lambda_{fs} + \lambda_i + \lambda_0 + \lambda_c r \cos(\psi_k) + \lambda_s r \sin(\psi_k) \quad (2)$$

where the quantities λ_0 , λ_s , and λ_c are small time varying perturbations. In the dynamic inflow model, the perturbation quantities in the inflow are related to the perturbation aerodynamic forces and moments on the rotor through the following system of linear differential equations [11,12,13].

$$M_{\lambda\lambda} \begin{bmatrix} \dot{\lambda}_0 \\ \dot{\lambda}_s \\ \dot{\lambda}_c \end{bmatrix} + L^{-1} \begin{bmatrix} \lambda_0 \\ \lambda_s \\ \lambda_c \end{bmatrix} = \begin{bmatrix} \Delta C_T \\ -\Delta C_{Mx} \\ \Delta C_{My} \end{bmatrix} \quad (3)$$

The forcing terms on the right hand side are the perturbations in the aerodynamic thrust force, roll moment, and pitch moment applied to the rotor hub. The actual values of the matrices in the equation depend on assumptions made during their derivation. In this paper we use the model from Ref. 13 as defined by

$$M_{\lambda\lambda} = \text{diag} \left[\frac{128}{75\pi}, -\frac{16}{45\pi}, -\frac{16}{45\pi} \right] \quad (4)$$

$$L = \frac{1}{v} \begin{bmatrix} \frac{1}{2} & 0 & \frac{15}{64}\pi \sqrt{\frac{1-\sin(\alpha)}{1+\sin(\alpha)}} \\ 0 & \frac{-4}{1+\sin(\alpha)} & 0 \\ \frac{15}{64}\pi \sqrt{\frac{1-\sin(\alpha)}{1+\sin(\alpha)}} & 0 & \frac{-4}{1+\sin(\alpha)} \end{bmatrix} \quad (5)$$

where $\alpha = \tan^{-1} \left(\frac{\lambda}{\mu} \right)$ and $v = \frac{\mu^2 + \lambda(\lambda + \lambda_i)}{\sqrt{\mu^2 + \lambda^2}}$.

The equations of motion of the coupled rotor/fuselage system are very lengthy and contain geometrically nonlinear terms due to moderate blade deflections in the aerodynamic, inertial, and structural forces. Furthermore, the coupled rotor/fuselage equations have additional complexity due to the presence of the fuselage degrees of freedom. To reduce the equations to a manageable size, an ordering scheme is used in the derivation of the equations of motion to systematically remove the higher order nonlinear terms [14]. The ordering scheme is based on the assumption that

$$1 + O(\epsilon^2) \approx 1 \quad (6)$$

This simply states that terms of order ϵ^2 are negligible relative to terms of order unity. The quantity ϵ is a nondimensional parameter, which quantifies the meaning of a "small" term. For our purposes, it represents the slopes of the deflections of the blades, which usually are of an order of magnitude which is less than .15.

The equations of motion are derived using basic Newtonian mechanics. Although this approach is more cumbersome than analytical methods such as a Lagrangian approach, it is still used since some forces of the equations of motion have been derived in Ref. 7, and this provided a useful check. A symbolic manipulation program is used to generate the nonlinear set of equations of the rotor/fuselage system. Five fuselage equations result of which three enforce the fuselage translational equilibrium. The three resulting rotor blade equations are associated with the flap, lag, and torsional motions of each blade. Also, the aerodynamic thrust and roll moments at the hub center are determined for the perturbation aerodynamics in the dynamic inflow equation [22].

Trim and Stability

The stability of the system is determined through the linearization of the equations of motion about an equilibrium solution at a given trim condition of the helicopter. The process of trimming the helicopter and establishing the equilibrium solution is done by satisfying two sets of equations. One set of equations are the k^{th} rotor blade equations represented by

$$f_b(q_b, \dot{q}_b, \ddot{q}_b, q_t; \psi) = 0 \quad (7)$$

The vector f_b represents the flap, lead-lag, and torsion blade equations, where the inflow is assumed to be constant (i.e., $\lambda_k = \lambda$) and all of the fuselage degrees of freedom are set identically to zero. The vector q_t represents the *trim solution* for the flap, lag and torsion blade degrees of freedom β_k , ζ_k , and ϕ_k . In hover, the equilibrium solution is independent of time, and in forward flight the solution is periodic. The other set of conditions necessary to find these variables come from satisfying the nonlinear equations represented by

$$f_t(q_b, \dot{q}_b, \ddot{q}_b, q_t; \psi) = 0 \quad (8)$$

The vector f_t represents the \hat{x}_1 , and \hat{z}_1 vertical plane force equilibrium and the pitch and roll moments acting on the entire helicopter. The side force in the \hat{y}_1 direction is not included in the trim. These force equations come from the fuselage translational and moment equations, where again, the inflow is constant and the fuselage degrees of freedom are set identically to zero. In addition, f_t contains an inflow equation, which determines the amount of downwash generated by the finite span rotor blades.

$$\lambda = \mu \tan(\alpha_R) + \frac{C_T}{2\sqrt{\mu^2 + \mu^2}} \quad (9)$$

This is a steady state result from the steady far field momentum equation [11]. The equations in f_t are all referenced to a non-rotating system, and consequently contain a constant component as well as N_b per revolution harmonics if all the blades are assumed identical. For trim to be established, it is only necessary to satisfy the constant component of Eq. (8). The N_b per revolution components are associated with the vibratory loads and are not part of trimming the vehicle. When Eq. (8) contains all fuselage equations, the trim is referred to as propulsive. When the force equilibrium equations are removed only the moment equilibrium conditions need to be satisfied. This trim condition is usually denoted as moment trim and represents the situation when a rotor is mounted on a support such as the wind tunnel test. In this paper, only propulsive trim is used. Cases with moment trim were considered in Ref. 22.

Two approaches are used to determine both the trim and the equilibrium solutions. The first of these methods is harmonic balance, which extracts the trim solution and equilibrium solutions simultaneously. A periodic solution q_b is desired, so we assume a periodic solution of N_H harmonics of the form

$$q_b = q_{b0} + \sum_{n=1}^{N_H} q_{bnc} \cos(n\psi_k) + q_{bns} \sin(n\psi_k) \quad (10)$$

where q_{b0} , q_{bnc} , and q_{bns} are vectors representing $(1 + 2N_H)N_{DOF}$ coefficients. The quantity N_{DOF} is the number of degrees of freedom in the blade

equations, which is three for a flap-lag-torsion system. The basic idea of harmonic balance is to use Eq. (10) in Eqs. (7) and (8) and convert them to the series representation

$$f_b = f_{b0} + \sum_{n=1}^{N_1} f_{bnc} \cos(n\psi_k) + f_{bns} \sin(n\psi_k) \quad (11)$$

$$f_t = f_{t0} + \sum_{n=1}^{N_2} f_{tnc} \cos(N_b \psi_k) + f_{tns} \sin(N_b \psi_k) \quad (12)$$

The integers N_1 and N_2 are the number of harmonics that arise from such a substitution and the coefficient vectors of these equations are functions of the coefficient vectors of Eq. (10) and the vector of trim variables q_t . Equation (12) must have only its constant component set to zero for straight and level trim to be established. Equation (11), however, requires that all of the coefficient vectors be zero for the blade equations to be satisfied. If the higher frequency coefficients are small, then a reasonable approximation to satisfying Eq. (11) is to set the first $(2N_H + 1)$ vectors of coefficients to zero. More compactly stated let

$$F(Q) = 0 \quad (13)$$

for trim to be satisfied, where

$$F \triangleq \begin{bmatrix} f_{b0} \\ f_{b1c} \\ f_{b1s} \\ \vdots \\ f_{bN_H c} \\ f_{bN_H s} \\ f_{t0} \end{bmatrix}; \quad Q \triangleq \begin{bmatrix} q_{b0} \\ q_{b1c} \\ q_{b1s} \\ \vdots \\ q_{bN_H c} \\ q_{bN_H s} \\ q_t \end{bmatrix}$$

The size of our equations prohibits such a procedure, so the formation of Eq. (13) is done by numerical means. Using the following relationships from Fourier analysis

$$f_{b0} = \frac{1}{2\pi} \int_0^{2\pi} f_b(q_b, \dot{q}_b, \ddot{q}_b, q_t; \psi) d\psi \quad (14)$$

$$f_{bnc} = \frac{1}{\pi} \int_0^{2\pi} f_b(q_b, \dot{q}_b, \ddot{q}_b, q_t; \psi) \cos(n\psi) d\psi \quad (15)$$

$$f_{bns} = \frac{1}{\pi} \int_0^{2\pi} f_b(q_b, \dot{q}_b, \ddot{q}_b, q_t; \psi) \sin(n\psi) d\psi \quad (16)$$

$$f_{t0} = \frac{1}{2\pi} \int_0^{2\pi} f_b(q_b, \dot{q}_b, \ddot{q}_b, q_t; \psi) d\psi \quad (17)$$

The vector F can be formed given a set of coefficients q_{b0} , q_{bnc} , q_{bns} , and q_t . This can be done numerically using one of the many integration procedures available. In this paper, Gaussian quadrature is used to reduce the number of integrand evaluation needed for a given accuracy [15]. Since the vector F can be evaluated given Q, the solution of Eq. (13) can be obtained using numerical techniques for solving systems of non-linear algebraic equations. In this paper, a Newton method using finite differences to form the Jacobian is used to extract this solution. The vector Q that satisfies Eq. (13) gives the trim condition and the equilibrium solution to a given number of harmonics.

The more conventional approach to trim is a two step procedure consisting of flap-trim and a separate rotor blade solution. Flap-trim is a simplification of the harmonic balance technique, where f_b contains *only* the equation associated with flap and q_b is *only* the flap degree of freedom. The trim solution and the flap equilibrium solution can be found as before but will, in certain respects, be too crude an approximation. The equilibrium solution in the flap degree of freedom that is generated by this technique is not accurate enough, and may give somewhat inaccurate stability results if it is used in linearizing the full equations. This is the consequence of only partially satisfying the set equations given by (7) and (8) when *all* the rotor degrees of freedom are present. To resolve this problem, Eq. (7) is solved with *all* the blade degrees of freedom present using the trim solution q_t from the flap-trim solution. The solution to the flap, lag and torsion differential equations in (7) is extracted using quasilinearization. This method uses the linearization of Eq. (7) in an iterative approach to converge on the periodic non-linear solution of Eq. (7). A detailed discussion of the method can be found in Refs. 16 and 17.

Using the trim and the equilibrium solution provided by either of the above techniques, the non-linear equations of motion can be linearized. This process is accomplished by using the first order Taylor expansion for all rotor fuselage, and inflow equations about the rotor equilibrium solution and gives a linear equation

$$[M(\psi)] \Delta \ddot{q} + [C(\psi)] \Delta \dot{q} + [K(\psi)] \Delta q + [N(\psi)] u = 0 \quad (18)$$

The elements of the M, C, K, and N matrices are the partial derivatives of the appropriate equation of motion with respect to the appropriate degree of freedom evaluated at the equilibrium solution. Therefore, these matrices are periodic in time and also depend on the equilibrium values of the blade in flap, lag and torsion.

A multi-blade coordinate transformation is applied to Eq. (18), which transforms the set of rotating blade degrees of freedom to a set of hub fixed non-rotating coordinates [18]. This transformation is introduced because the new coordinate system has distinct advantages over the rotating coordinate representation. The original system of Eq. (18) has coefficients with a fundamental frequency of unity, however, the transformed system has a higher fundamental frequency. These higher frequency periodic terms have a reduced influence on the behavior of the system and can be ignored in some analyses at low advance ratios [14]. In hover, the original system has periodic coefficients with a frequency of unity, but the transformed system has constant coefficients, which is a valuable simplification when determining the stability of the system. Furthermore, in hover, the transformation decouples the system into three groups; the collective modes and collective pitch input, the sine/cosine modes and sine/cosine pitch inputs, and the alternating modes with no input. This is relevant in the control design, since it indicates which controls affect (or do not affect) which modes. These uncoupled groups become more coupled and the periodic terms become increasingly more important as the advance ratio is increased.

Once the transformation is carried out, the system is rewritten in first order form.

$$\dot{x} = A(\psi)x + B(\psi)u \quad (19)$$

The fundamental frequency of the coefficient matrices depends on the number of rotor blades. For an odd bladed system the fundamental frequency is N_b per revolution, while for an even bladed system the fundamental frequency is $N_b/2$ per revolution [18]. Stability can now be determined using either an eigenvalue analysis or Floquet theory for the periodic problem in forward flight. An approximate stability analysis in forward flight is also possible by performing an eigen analysis on the constant coefficient portion of the system matrices of Eq. (19).

The mathematical model was carefully tested to verify that its results are consistent with other investigators' results. Figure 3 shows the lead-lag regressing damping obtained from this analysis compared to the experimental results of Ref. 19. In Ref. 19, the stability of a three bladed rotor/fuselage model was investigated experimentally, using a carefully constructed dynamic model of a three bladed rotor which was designed to behave like a spring restrained rigid blade model with flap and lag degrees of freedom. The rotor system was on a special mount allowing for pitch and roll motions and the experiment was conducted in hover only. Other comparisons were made to results from Refs. 8, 20, and 21 and for all cases good correlation was obtained [22].

The Nominal Configuration

The non-dimensional data of the configuration used in this study is presented in Table 1. The parameters are selected to make the nominal configuration somewhat similar to the MBB 105 helicopter in size and weight [23]. The nominal configuration differs from the MBB 105 in that it has an unstable air resonance mode, which was induced by adjustments in some rotor and body parameters. The system has 37 states. The five body degrees of

freedom and the twelve rotor degrees of freedom (three degrees of freedom for each blade) produce 34 position and rate states. The dynamic inflow model augments the system with three more states giving a total system order of 37. For the results that follow, the equilibrium solution is established with $N_H = 3$ in Eq. (10). This is sufficiently accurate for all of the constant approximation results (i.e. constant portion of A and B in Eq. (19)). For the periodic analysis at advance ratios from zero to 0.3, N_H is also three and one harmonic of frequency two is used for the coefficient matrices in Eq. (19). For advance ratios about 0.3, $N_H = 5$ and two harmonics of frequency two and four are used for the coefficient matrices in (19).

Table 1: Data of the nominal configuration.

Characteristic Dimensions

Blade mass = 52 kg
 Rotor radius = 4.9 m
 Rotor rate = 425 RPM

Rotor Data

1 = 0.85	e = 0.15	$\omega_{F1} = 1.15$ at zero pitch
$x_b = 0.36$	$\gamma = 5.0$	$\omega_{L1} = 0.620$
$I_b = 0.18$	$C_{d0} = 0.01$	$\omega_{T1} = 3.00$
$J_x = 0.00015$	a = 5.90	.5 percent damping
$J_y = 0.$	$x_A = 0.$	$\sigma = 0.07$
$J_z = 0.00015$	$y_b = 0.$	$R_c = 1.0$
$\beta_p = 0.$	b = 0.02749	$N_b = 4.0$
$\mu_{cruise} = .3$		

Fuselage Data

$M_F = 32.$	f = 0.60
$I_{Cxx} = 1.0$	$Z_{MH} = 0.2667$
$I_{Cyy} = 4.0$	$Z_{MC} = 0.0333$

Horizontal Tail Data

$X_{MT} = 1.0$	$a_T = 5.0$
$S_T = 0.04$	$C_{d0T} = 0.007$
AR = 5.5	

Figure 4 shows the pole locations in the s-plane of some of the modes of the full model at $\mu = 0.3$. The lead-lag regressing mode is the air resonance instability and is mildly unstable in this flight condition. Figure 5 shows the air resonance damping of the configuration with and without dynamic inflow at various advance ratios. Two curves are shown for each of

these cases reflecting an eigen analysis on the constant coefficient system and a Floquet analysis on the periodic system. The stabilizing effect of forward flight, which is shown in the figure is consistent with experimental observation [24]. For hover, the system has constant coefficients and thus the two analyses should give precisely the same results as is clearly evident in the figure. It should be noted that this property is used as an additional check of the numerical accuracy of the integration scheme used in the Floquet analysis. The quasi-steady analysis is more stable than the unsteady analysis and a considerable difference exists between the models at low advance ratios.

Figure 6 shows that neglecting the torsional degree of freedom on the nominal configuration increases the instability of the lead-lag regressing mode. The trend of the two curves also tends to diverge at high advance ratios. The addition of torsion also tends to amplify the effect of the periodic terms. At high values of advance ratio, the flap-lag-torsion model shows a much greater difference between the constant and periodic stability analysis than does the flap-lag analysis.

The effect on the trim solution of using flap-trim and harmonic balance in full trim is depicted in Figure 7. The rotor tilt angle and the inflow of the two approaches are identical, but the swashplate inputs are slightly different. The largest difference arises in the collective input with the full trim procedure giving a larger collective input angle. This small difference in trim inputs can strongly affect the response of the blade as can be seen in Figure 8. Although the torsion and lead-lag motion are not strongly affected, the flap response is greatly attenuated by using the full trim procedure. The trim solution plays a less significant roll in the air resonance damping as seen in Figure 9. The harmonic balance solution produces slightly more stability than the flap-trim with quasilinearization solution, which is consistent with the results of Ref. 25.

State Feedback Active Control

To assess the air resonance control problem the deterministic linear optimal regulator is used to stabilize the air resonance instability of the nominal configuration. In summary, the regulator problem gives the control that minimizes the cost functional [26].

$$J = \frac{1}{2} \int_0^{T_f} x^T H^T H x + u^T R u \, dt \quad \text{as} \quad T_f \rightarrow \infty \quad (20)$$

The vector x are the states of the system and are constrained by the system in Eq. (19). The vector u represents the control inputs, which for this problem are the collective, sin, and cosine pitch inputs. The matrices H and R are chosen by the designer and the matrix R must be a positive definite symmetric matrix. For the following studies, the state weight matrix is chosen such that

$$x^T H^T H x = .3^2 [\beta_{1c}^2 + \beta_{1s}^2 + \zeta_{1c}^2 + \zeta_{1s}^2 + \dot{\beta}_{1c}^2 + \dot{\beta}_{1s}^2 + \dot{\zeta}_{1c}^2 + \dot{\zeta}_{1s}^2 + R_{Mx}^2 + R_{My}^2 + R_{Mz}^2 + \dot{R}_{Mx}^2 + \dot{R}_{My}^2 + \dot{R}_{Mz}^2 + \theta_x^2 + \theta_y^2 + \dot{\theta}_x^2 + \dot{\theta}_y^2] \quad (21)$$

The weight matrix is chosen to only weigh the sine and cosine terms of flap and lead-lag degrees of freedom as well as the fuselage degrees of freedom. The torsional degrees of freedom and the inflow degrees of freedom are not weighed since they will eventually be removed during the subsequent studies. The R matrix is set to the identity.

For the periodic system equations, the solution to the problem is given by the feedback law

$$u_{opt} = -K_c(\psi)x \quad (22)$$

where

$$K_c(\psi) = R^{-1}B(\psi)^T P_c(\psi) \quad (23)$$

The matrix P_c is the positive definite steady periodic solution to the Riccati equation

$$A(\psi)^T P_c(\psi) + P_c(\psi)A(\psi) + H^T H - P_c(\psi)B(\psi)R^{-1}B(\psi)^T P_c(\psi) = -\dot{P}_c(\psi) \quad (24)$$

For constant system equations, the gain is constant and is found by solving the algebraic Riccati equation, which is Eq. (24) with the right hand side set to zero and all other matrices constant. For both constant and periodic systems, uniqueness and existence of the positive semi-definite solution of Eq. (24) is assured if the pair (A,B) is stabilizable and the pair (A,H) is detectable [26,27]. In short, stabilizable means that any uncontrollable portion of the system must be stable. Finally, the closed loop system given by

$$A_{c1}(\psi) = (A(\psi) - B(\psi)K_c(\psi)) \quad (25)$$

will be stable.

Though the mathematical definitions of stabilizability and detectability of a periodic system are readily available, reliable numerical techniques for determining these conditions on practical systems (i.e. large systems) are not. Due to the lack of algorithms for checking periodic controllability, this check is restricted to the constant coefficient portion of the system. The model is constant in hover, so this restriction is considered a reasonable approximation for low advance ratios.

For time invariant systems, tests for controllability abound [28], but few are reliable for moderately sized systems. The most common test for controllability given by the statement

$$\text{Rank } [B \mid AB \mid A^2B \mid A^3B \mid \dots \mid A^{n-1}B] = n \quad (26)$$

fails dismally with the 37th order system of this paper. The test used in this paper is the algorithm described in Ref. 28 and is a reliable means of checking controllability of moderately sized systems. The test uses a series of Householder transformations to transform the system into block Hessenberg form where controllability can be easily determined. An added feature of the method is that, as it iterates through its cycles, it transforms the system into control canonical form (i.e. the controllable modes of the system are decoupled from the uncontrollable modes). Stabilizability is then a simple check of the stability of the uncontrollable portion of the system. As a check of the reliability of the method on our large system, the controllability of the system was checked in hover, since it is known that the alternating modes are uncontrollable. This uncontrollability showed itself affirming the numerical reliability of the method on large systems and revealing that no other modes were uncontrollable. In forward flight, the system becomes completely controllable (in a constant coefficient sense), which is reasonable due to the coupling effect of forward flight on the alternating modes. Thus, in forward flight, all modes can be theoretically controlled with the given set of swashplate inputs. In hover, these inputs will be unable to control the alternating modes. Of these modes, only the inplane alternating mode has the realistic potential for instability and generally occurs with stiff-in-plane rotors [29,30]. Since air resonance affects only soft-in-plane systems, it is unnecessary to have any control over this mode.

The solution of the algebraic Riccati equation is extracted using the method devised by Potter [31]. This method uses the eigen data of the Hamiltonian matrix associated with matrix Riccati equation and it is fairly inexpensive taking approximately two seconds to find the solution to a 37th order system. The periodic Riccati equation is solved using the method discussed in Ref. 32. This method uses the eigen data of the state transition matrix of the Hamiltonian matrix. Essentially this method is the periodic extension to the constant matrix Riccati solver of Ref. 31. The method is fairly expensive taking approximately 250 seconds of computer time to get a solution to the 37th order system using one harmonic.

Active Control Numerical Results

All of the closed loop results presented in this section are based on the previously described nominal configuration with feedback determined from the linear optimal regulator. The nominal system is constant in the hover condition and becomes periodic in forward flight, which is the result of applying the multi-blade coordinate transformation. The first effect that is examined is the effect of these periodic terms on the closed loop lead-lag regressing damping for three cases. The curve designated "Periodic Optimal" is the closed loop damping when the full periodic system is used to calculate periodic feedback gains. This case represents the optimal solution when all dynamics are present. The curve "Constant Optimal" is the

closed loop damping when the approximate constant coefficient model is used to calculate constant feedback gains and these gains are applied to the constant model. This solution would result if a constant model were used in the design of the controller. The curve "Constant on Periodic" is the closed loop damping from applying the constant gains from the constant model to the fully periodic model. All of the curves are identical near hover and show a small deviation from one another only at the higher advance ratios. This simple study suggests that the periodic terms in the system equations do not greatly affect the closed loop damping of the air resonance mode and that a constant analysis is possible in the initial design phase of an air resonance controller. Considering the cost of extracting a periodic feedback gain from the time varying matrix Riccati equation, the remaining studies of this paper are restricted to the constant approximation of the system equations.

The next modeling effect studied is the role of the unsteady aerodynamics on the full state feedback control. Figure 11 shows the closed loop damping of the lead-lag regressing mode using three feedback gains. The curve designated "DI Optimal" is the optimal damping resulting from feedback gains that are calculated from the full model and applied to this same model. This damping represents the "best" we can do given that our full model is indeed the "real" model. The curve "QS Optimal" is the damping that results from a feedback based on a quasisteady (i.e. no dynamic inflow) aerodynamic model placed on itself. This curve represents what really occurs when the controller based on quasi-steady aerodynamics is applied to the fully unsteady system. Though the curves show similar trend behavior, significant differences in damping exist. A much lower level of stability (50 percent) occurs when a quasi-steady design model is used on the full model.

Another often neglected effect in rotor/fuselage analyses is the effect of the torsional degree of freedom on the blade dynamics. Figure 12 shows this effect on the closed loop lead-lag regressing damping. The designation of the curves is similar to the dynamic inflow study, but now we refer to the presence or absence of the torsional degree of freedom. Both the "F-L-T Optimal" and the "F-L Optimal" damping are within 10 percent of each other, though a 25 percent increase in damping occurs when the "F-L Optimal" gain is applied to the full system. Though using the flap-lag design model is conservative, giving more damping when applied to the flap-lag torsion model, one cannot conclude this will always be the case. The reverse could occur if the open loop flap-lag damping is more stable than the flap-lag-torsion damping and this depends on the operating condition of the system.

The effect of the trim solution is examined using the two approaches available to extract a trim setting and equilibrium solution. Figure 13 shows the closed loop lead-lag regressing damping using full state feedback. The curve designated "HB Optimal" is the solution using the harmonic balance trim procedure while the curve designated "QL Optimal" is the solution using flap-trim with quasilinearization. The curve "QL on HB" is the case when the gains from "QL Optimal" are applied to the full model. Full trim does not appear essential, since all curves lie within 10 percent of each other. The numerical cost of using either technique is almost the same, so, harmonic balance is preferable if available.

The system as it is has three inputs for controlling the air resonance mode. It is known that collective input is decoupled from this mode in the

hover condition, and eventually couples with this mode as the advance ratio is increased. A reasonable area of investigation is to determine how much effect the collective control has on controlling the unstable mode in forward flight. The controllability of the system was checked with only the sine and cosine inputs, and this showed the only mode that was uncontrollable (though stabilizable) was the vertical translational mode. Figure 14 shows two curves of closed loop-lead-lag regressing damping. One curve is the damping with the collective input and the other is the damping without this input. The hover condition gives identical results due to the decoupling of the collective input. At the highest advance ratio, a 10 percent reduction in damping occurs, which is fairly small degradation in performance. This study suggests that the collective mode is only of marginal value in controlling the air resonance mode in forward flight.

In Ref. 4, the author suggested using partial state feedback of the body degrees of freedom as a simple and implementable means of controlling ground resonance of an articulated rotor system. In this reference, it was demonstrated that using only the optimal gains associated with body modes gives a reasonable level of stability to the system in hover. Given this, the author concluded that this would be a reasonable control implementation requiring only a few body state measurements. Along these same lines, a comparison of full state feedback is made to partial state feedback using the body degrees of freedom. The optimal gain matrix from the full state feedback is used with all elements set to zero except those associated with the body position rate coordinates. Figure 15 shows the lead-lag regressing damping for this case along with the full state feedback damping. A severe drop in damping is seen and the system becomes unstable for most of the forward flight region. Additionally, the use of only the body feedback gains tends to destabilize the lead-lag progressing damping shown in Figure 16. In the previous studies, this mode showed no tendency towards instability, but in this case the mode is strongly destabilized. This clearly shows that partial state feedback of the body modes is inadequate for control of the air resonance instability.

Finally it should be noted that full state feedback is not a particularly practical method for suppressing the air resonance instability. A more practical method for suppressing this instability was described in Refs. 22 and 33. The controller design [33] is a simple multivariable compensator using conventional swashplate inputs and a single body roll rate measurement. The controller design is based on a linear estimator in conjunction with optimal feedback gains, and the design is done in the frequency domain using the Loop Transfer Recovery method [34,35]. The controller is shown to suppress the air resonance instability throughout a wide range of helicopter loading conditions and forward flight speeds.

Concluding Remarks

A coupled rotor/fuselage model was presented containing low frequency unsteady aerodynamic effects, blade torsional dynamics, in forward flight, which are effects that have been neglected in previous studies of active control of air resonance. Furthermore, a new trim procedure was implemented in which full coupling between the trim variables and the aeroelastic equilibrium solution variables is achieved. The model was carefully validated by comparing results with the analytical and experimental results of

other independent investigators. The coupled rotor/fuselage system was combined with a linear quadratic optimal control theory to design full state feedback controllers. These controllers were then used to evaluate the importance of various modeling effects on the closed loop damping of the unstable air resonance mode. Periodic terms in the model seem to play only a small role at advance ratios less than .4. With this in mind and considering the cost of extracting periodic gains, it seems reasonable to neglect the periodic terms in the initial stage of controller development. Knowing that the constant model is a reasonable approximation also allows the use of many other control design techniques. Unsteady aerodynamics and blade torsional flexibility seem to be important modeling effects that should be included in a controller design model. Significant errors between 25 to 50 percent in closed loop lead-lag damping could result if these effects are not included. The difference between using a full trim technique and using flap-trim with quasilinearization is marginal giving ten percent error in open and closed loop lead-lag regressing damping. However, significant differences arise in the flap response of the blade when using these two different procedures suggesting the type of trim is more important in the blade response problem. The collective control input seems to have little influence in controlling air resonance at high advance ratios, so it is felt to be unnecessary to complete the control task. Finally, partial state feedback of the body states does not seem to be a reasonable approach to controlling air resonance. Poor lead-lag damping results and lead-lag progressive mode excitation is a possible consequence. A practical controller design based on a simple multivariable compensator using conventional swashplate input and a single body roll rate measurement was presented in Ref. 33 which represents a sequel to the study presented in this paper.

Acknowledgment

This research was funded by NASA Ames Research Center, Moffett Field, CA under Grants NAG 2-209 and NAG-477. The constructive comments of the grant monitor, Mr. S Jacklin are hereby gratefully acknowledged.

References

1. Burkham, J.E., and Miao, W., "Exploration of Aeroelastic Stability Boundaries with a Soft-in-plane Hingeless Rotor Model," *Journal of the American Helicopter Society*, Vol. 17, No. 4, Oct. 1972, pp. 27-35.
2. Donham, R.E., Cardinale, S.V., and Sachs, I.B., "Ground and Air Resonance Characteristics of a Soft Inplane Rigid Rotor System," *Journal of the American Helicopter Society*, Vol. 14, No. 4, Oct. 1969, pp. 33-41.
3. Straub, F.K., and Warmbrodt, W., "The Use of Active Controls to Augment Rotor/Fuselage Stability," *Journal of the American Helicopter Society*, Vol. 30, No. 3, July 1985, pp. 13-22.
4. Straub, F.K., "Optimal Control of Helicopter Aeromechanical Stability," *Vertica*, Vol. 11, No. 3, 1987, pp. 425-435.
5. Young, M.I., Bailey, D.J. and Hirschbien, M.S., "Open and Closed Loop Stability of Hingeless Rotor Helicopter Air and Ground Resonance," Paper No. 20, NASA-SP 352, 1974.

6. Greenberg, J.M., "Airfoil in Sinusoidal Motion in a Pulsating Stream," NACA-TN 1326, 1947.
7. Venkatesan, C., and Friedmann, P., "Aeroelastic Effects in Multi-Rotor Vehicles with Applications to a Heavy-Lift System," NASA-CR 3822, Aug. 1984.
8. Dinyavari, M.A.H., and Friedmann, P.P., "Application of Time Domain Unsteady Aerodynamics to Rotary-Wing Aeroelasticity," *AIAA Journal*, Vol. 24, No. 9, 1987, pp. 1424-1432.
9. Friedmann, P.P., and Venkatesan, C., "Influence of Unsteady Aerodynamic Models on Aeromechanical Stability in Ground Resonance," *Journal of the American Helicopter Society*, Vol. 31, No. 1, Jan. 1986, pp. 65-74.
10. Gaonkar, G.H., and Peters, D.A., "Effectiveness of Current Dynamic Inflow Models in Hover and Forward Flight," *Journal of the American Helicopter Society*, Vol. 31, No. 2, April 1986, pp. 47-57.
11. Johnson, W., *Helicopter Theory*, Princeton University Press, 1980.
12. Peters, D.A., and Gaonkar, G.H., "Theoretical Flap-Lag Damping with Various Dynamic Inflow Models," *Journal of the American Helicopter Society*, Vol. 25, No. 3, July 1980, pp. 29-36.
13. Pitt, D.M., and Peters, D.A., "Theoretical Predictions of Dynamic Inflow Derivatives," *Vertica*, Vol. 5, 1981, pp. 21-34.
14. Friedmann, P.P., "Formulation and Solution of Rotary-Wing Aeroelastic Stability and Response Problems," *Vertica*, Vol. 7, No. 2, 1983, pp. 101-141.
15. Carnahan, B., Luther, H.A., and Wilkes, J.O., *Applied Numerical Methods*, John Wiley and Sons, Inc., New York, 1969.
16. Friedmann, P.P., and Kottapalli, S.B.R., "Coupled-Flap-Lag-Torsion Dynamics of Hingeless Rotor Blades in Forward Flight," *Journal of the American Helicopter Society*, Oct. 1982, pp. 28-36.
17. Celi, R., and Friedmann, P.P. "Use of an Implicit Formulation Based on Quasilinearization for the Aeroelastic Response and Stability of Rotor Blades in Forward Flight," AIAA Paper 87-0921-CP, Proc. AIAA/ASME/ASCE/AHS Structures, Structural Dynamics and Materials Conf., Part 2b, Monterey, CA, April 9-10, 1987, pp. 730-742.
18. Hohenemeser, K.H., and Ying, Sheng-Kuang, "Some Applications of the Method of Multi-Blade Coordinates," *Journal of the American Helicopter Society*, Vol. 17, No. 4, 1972, pp. 1-12.
19. Bousman, W.G., "An Experimental Investigation of the Effects of Aeroelastic Coupling on Aeromechanical Stability of a Hingeless Rotor Helicopter," *Journal of the American Helicopter Society*, Vol. 26, No. 1, Jan. 1981, pp. 46-54.
20. Nagabushanam, J., and Gaonkar, G.H., "Rotorcraft Air Resonance in Forward Flight with Various Dynamic Inflow Models and Aeroelastic Couplings," *Vertica*, Vol. 8, No. 4, 1984, pp. 373-394.

21. Panda, B. and Chopra, I., "Flap-Lag-Torsion Stability in Forward Flight," *Journal of the American Helicopter Society*, Vol. 30, No. 4, Oct. 1985.
22. Takahashi, M.D., "Active Control of Helicopter Aeromechanical and Aeroelastic Instabilities," Ph.D. Dissertation, Mechanical, Aerospace and Nuclear Engineering Department, University of California, Los Angeles, June 1988.
23. Staley, J.A., "Validation of Rotorcraft Flight Simulation Program Through Correlation with Flight Data for Soft-in-Plane Hingeless Rotors," USAAMRDL-TR-75-50, Jan. 1976.
24. King, S.P., "Theoretical and Experimental Investigations into Helicopter Air Resonance," 39th Annual Forum of the American Helicopter Society, St. Louis, MO, May 9-11, 1983.
25. Reddy, T.S.R., and Warmbrodt, W., "Forward Flight Aeroelastic Stability from Symbolically Generated Equations," *Journal of the American Helicopter Society*, Vol. 31, No. 3, July 1986, pp. 35-44.
26. Kwakernaak, H., and Sivan, R., *Linear Optimal Control Systems*, John Wiley & Sons, Inc., New York, 1972.
27. Bittanti, S., Colaneri, P., and Guardabassi, G., "Analysis of Periodic Lyapunov and Riccati Equations via Canonical Decomposition," *Journal SIAM Control and Optimization*, Vol. 24, No. 6, November 1986, pp. 1138-1149.
28. Chen, C.T., *Linear System Theory and Design*, Holt, Rinehart, and Winston, New York, 1984, Chapter 5.
29. Anderson, W.D., "Investigation of Reactionless Mode Stability Characteristics of Soft Inplane Hingeless Rotor System," 29th Annual Forum of the American Helicopter Society, Washington, DC, May 1973.
30. Johnston, J.F., and Conner, F., "The Reactionless Inplane Mode of Stiff Inplane Hingeless Rotors," Lockheed Report LR26214 Lockheed California Co., Burbank, CA., Dec. 1973.
31. Potter, J.E., "Matrix Quadratic Solutions," *Journal SIAM Applied Math.*, Vol. 14, No. 3, May 1966, pp. 496-501.
32. Nishimura, T., "Spectral Factorization in Periodically Time-Varying Systems and Application to Navigation Problems," *AIAA Journal of Spacecraft*, Vol. 9, No. 7, July, 1972, pp. 540-546.
33. Takahashi, M.D. and Friedmann, P.P., "Design of a Simple Active Controller to Suppress Helicopter Air Resonances," Proc. 44th Annual Forum of the American Helicopter Society, June 16-18, 1988, pp. 305-316.
34. Doyle, J.C. and Stein, G., "Multivariable Feedback Design: Concepts for a Classical/Modern Synthesis," *IEEE Trans. on Automatic Control*, Vol. AC-26, No. 1, Feb. 1981, pp. 4-16.

35. Stein, G., "The LQG/LTR Procedure for Multivariable Feedback Control Design," *IEEE Trans. on Automatic Control*, Vol. AC-32, No. 2, Feb. 1987, pp. 105-114.

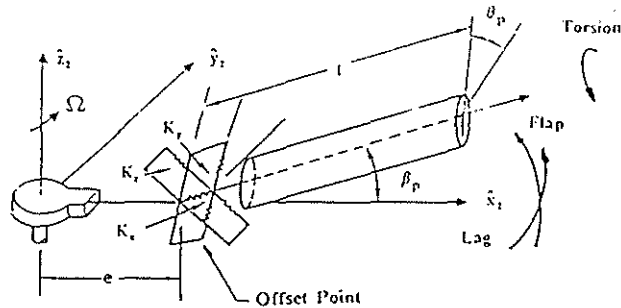


Figure 1: Offset hinged spring restrained blade model.

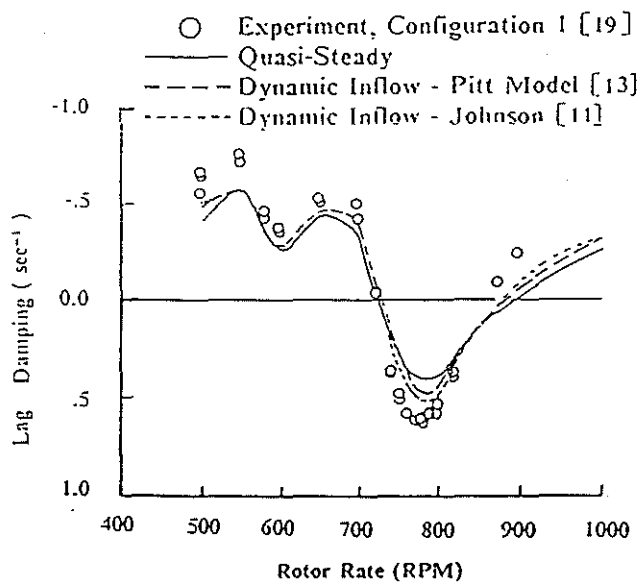


Figure 3: Lead-lag regressing damping of a rotor/fuselage system in hover at nine degrees blade pitch.

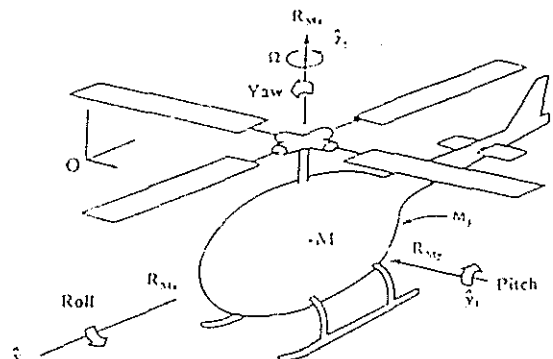


Figure 2: Rotor/fuselage configuration.

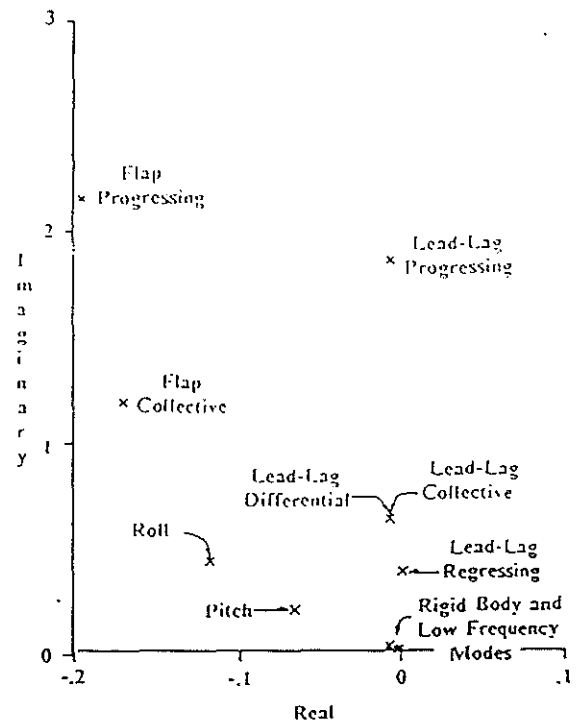


Figure 4: Some open-loop poles of the full constant model at advance ratio 0.3.

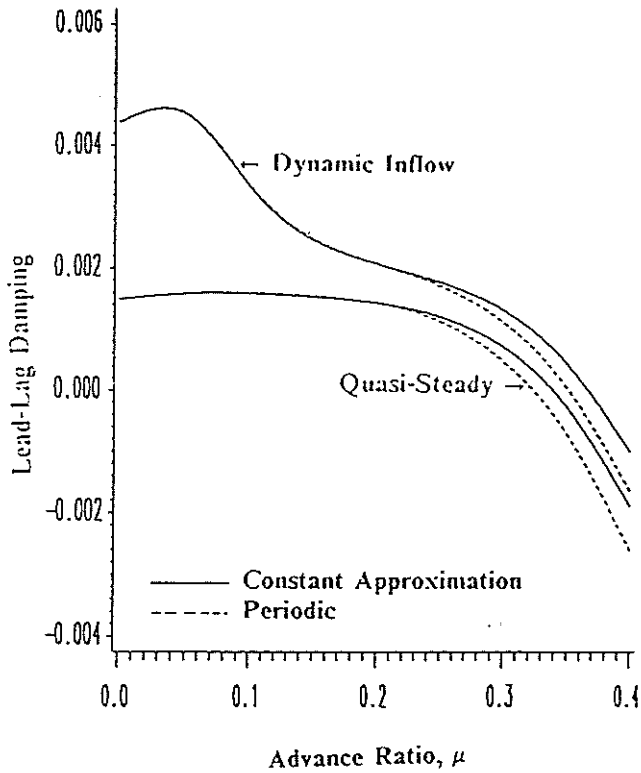


Figure 5: Open-loop lead-lag regressing damping of the nominal configuration with and without dynamic inflow.

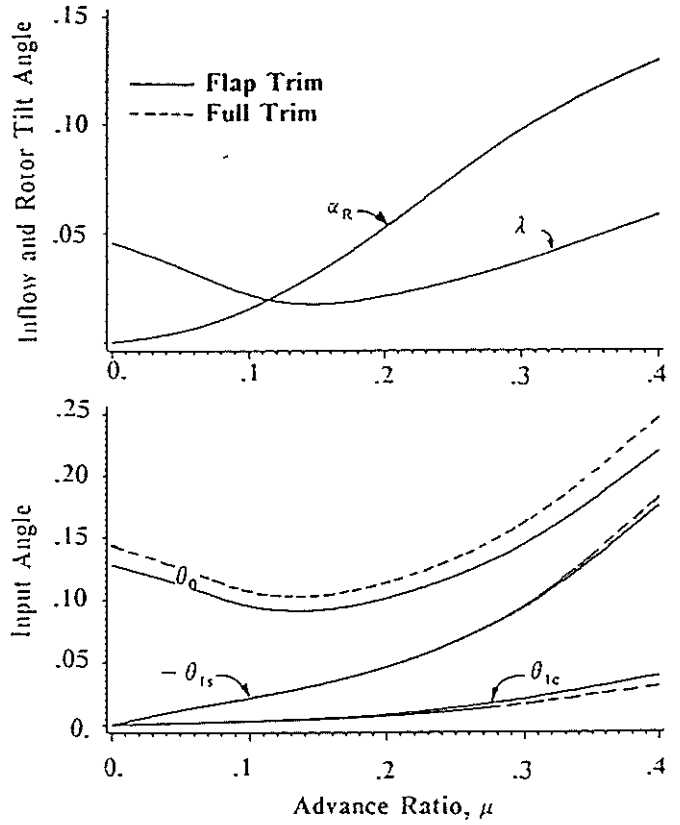


Figure 7: Harmonic balance full trim compared to flap-trim of the nominal configuration.

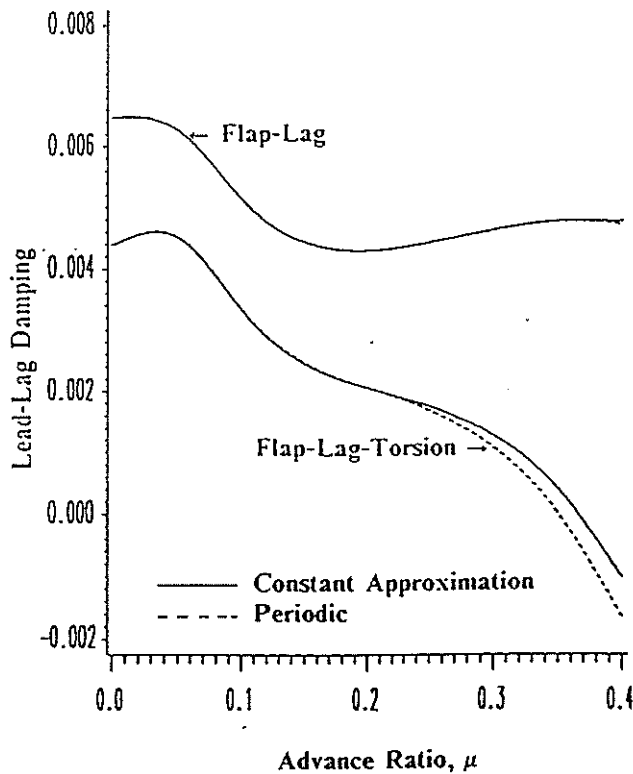


Figure 6: Open-loop lead-lag regressing damping of the nominal configuration with and without torsional blade flexibility.

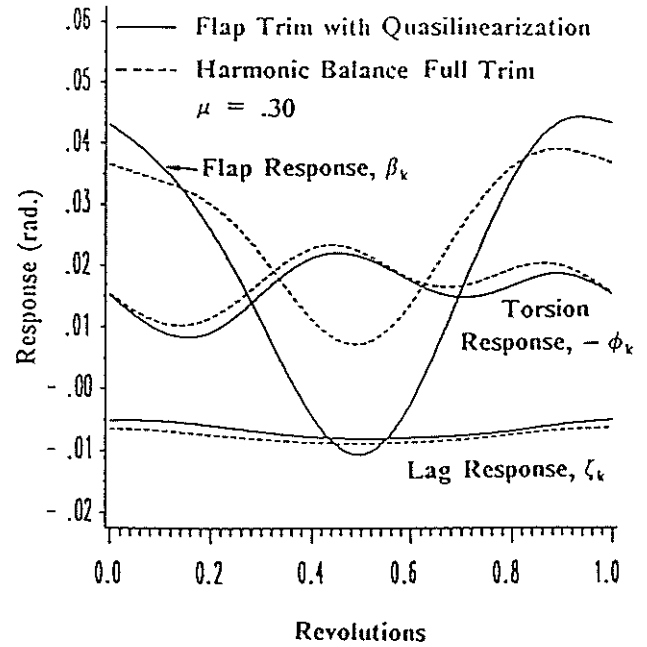


Figure 8: Equilibrium solutions from the harmonic balance full trim and the flap-trim with quasilinearization.

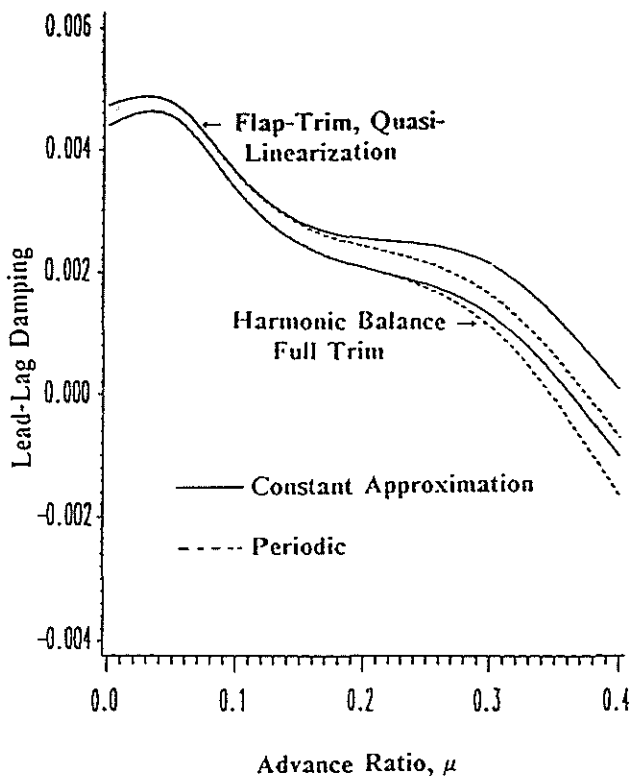


Figure 9: Open-loop lead-lag regressing damping of the nominal configuration using harmonic balance and flap-trim with quasilinearization.

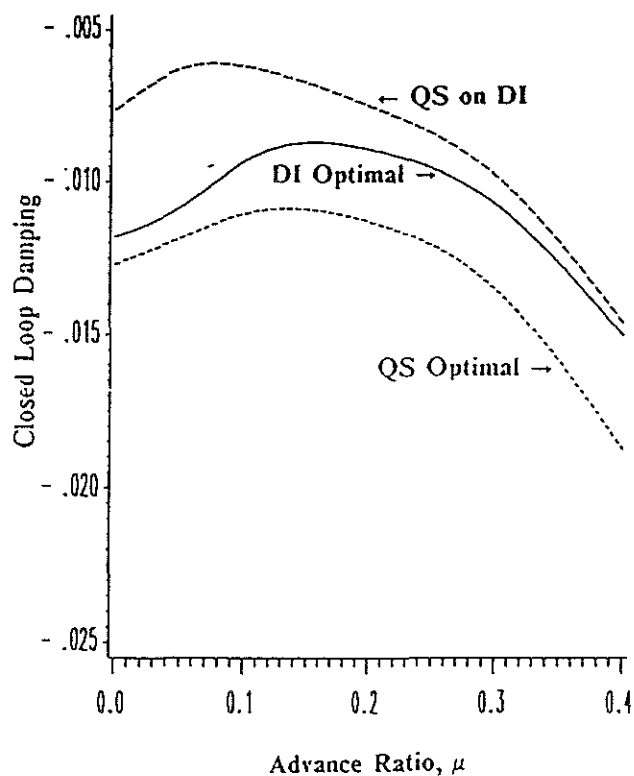


Figure 11: Closed-loop lead-lag regressing damping using a design model with and without dynamic inflow.

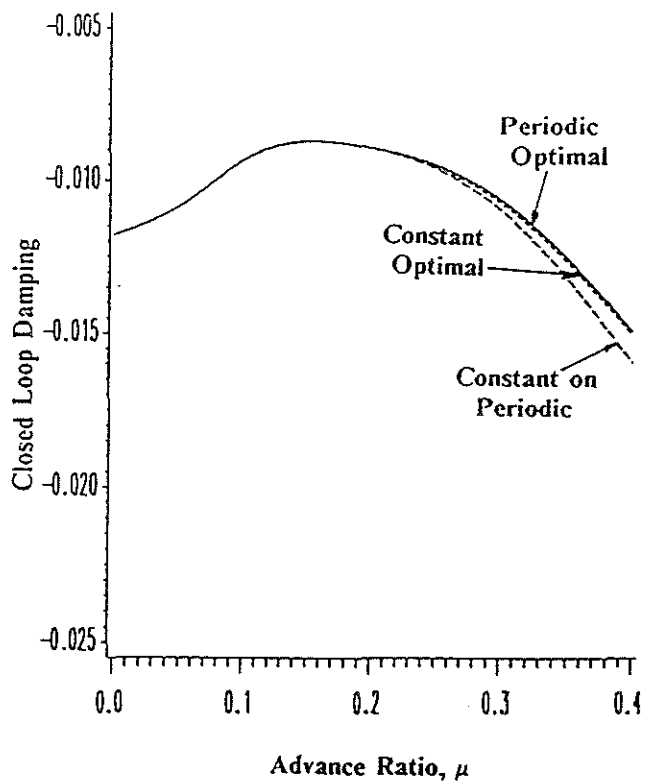


Figure 10: Closed-loop lead-lag regressing damping using a constant and periodic design model.

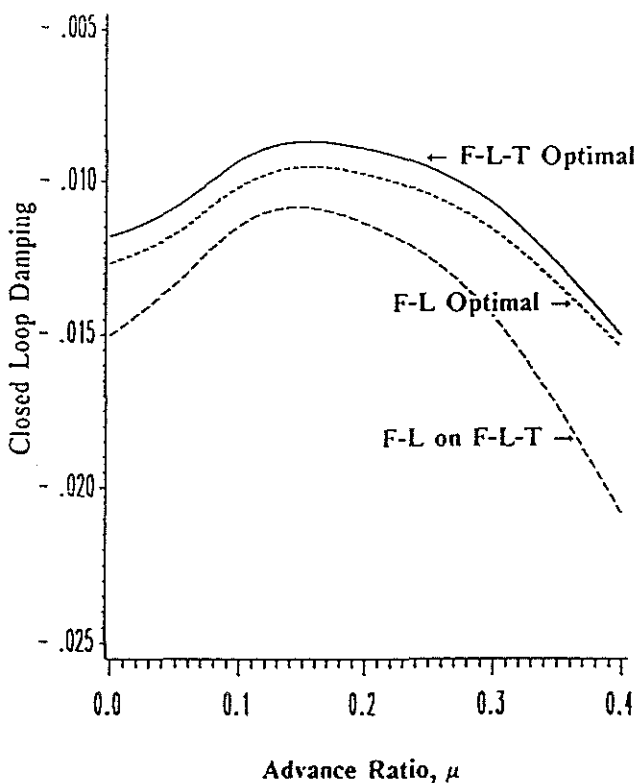


Figure 12: Closed-loop lead-lag regressing damping using a design model with and without torsional effects.

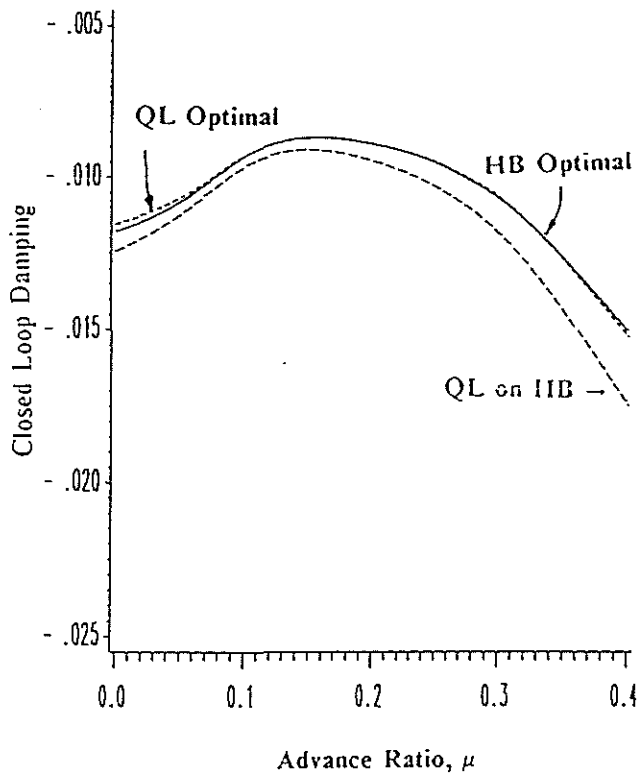


Figure 13: Closed-loop lead-lag regressing damping using a design model with harmonic balance trim and flap-trim with quasilinearization.

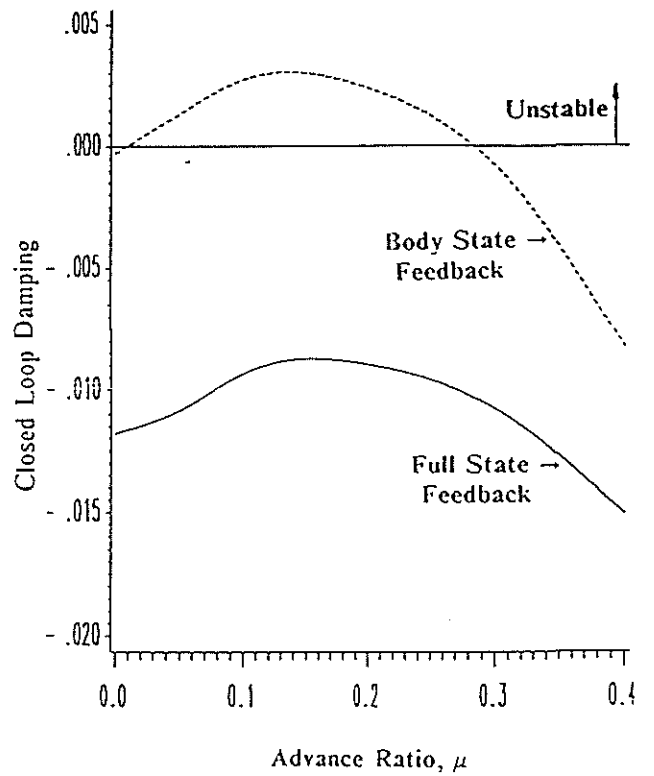


Figure 15: Closed loop lead-lag regressing damping using full and partial state feedback.

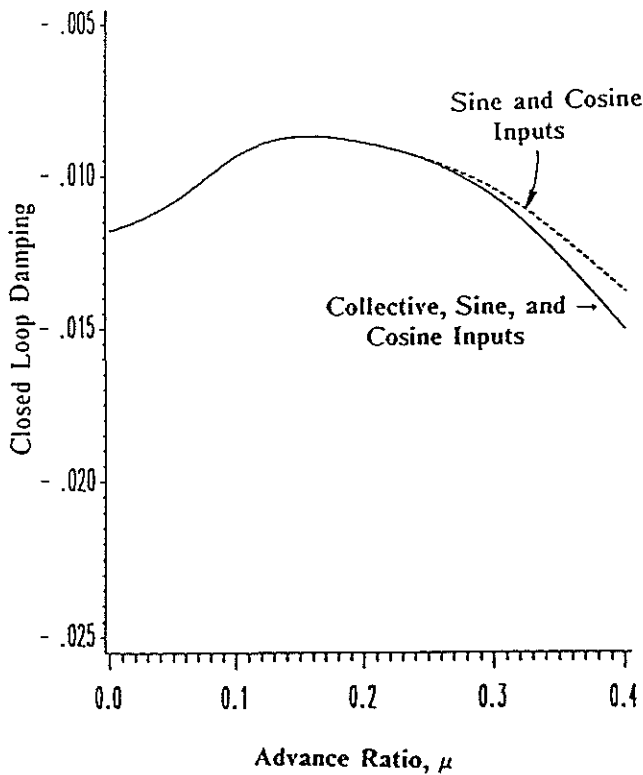


Figure 14: Closed loop lead-lag regressing damping with and without the collective pitch input.

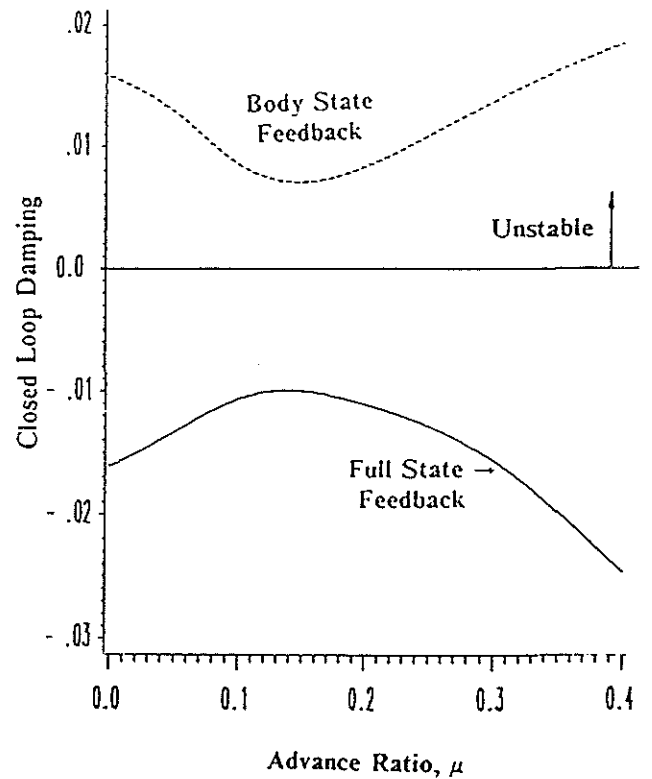


Figure 16: Closed loop lead-lag progressing damping using full and partial state feedback.